

Bathorhodopsin intermediates from 11-*cis*-rhodopsin and 9-*cis*-rhodopsin

(visual pigments/picosecond spectroscopy)

J. D. SPALINK*, A. H. REYNOLDS*, P. M. RENTZEPIS*[†], W. SPERLING[‡], AND M. L. APPLEBURY[§]

*Bell Laboratories, Murray Hill, New Jersey 07974; [‡]Institut fuer Neurobiologie, KFA Juelich, D-517 Juelich, Federal Republic of Germany; and [§]Department of Biological Sciences, Purdue University, West Lafayette, Indiana 47907

Contributed by P. M. Rentzepis, December 3, 1982

ABSTRACT Bathorhodopsin–rhodopsin difference spectra of native 11-*cis*-rhodopsin and regenerated 9-*cis*-rhodopsin were measured at room temperature with a double-beam laser spectrophotometer after excitation at 532 nm. A detailed analysis of data obtained at 85 psec after excitation suggests that the bathorhodopsins generated from 11-*cis*- and 9-*cis*-rhodopsin differ in their extinction coefficients and that their absorption maxima are shifted in wavelength by about 10 nm from one another. The ratio of quantum yields for photochemical production of the 11-*cis*-bathorhodopsin and the 9-*cis*-bathorhodopsin approximates 1. Implications that the early photochemical processes in vision are more complex than previously considered are explored.

An improved double-beam laser spectrophotometer was developed to perform a comparative study of the bathorhodopsin photoproducts of native 11-*cis*-rhodopsin and regenerated 9-*cis*-rhodopsin. The instrument measures difference spectra of the initial photoproduct (bathorhodopsin) minus the rhodopsin converted for each of these visual pigments under identical experimental conditions. Each spectrum, covering the range of 400–650 nm, was recorded with a single monitoring pulse after excitation at 532 nm. Particular attention was given to optimizing the signal-to-noise ratio of measured absorbance changes in order to achieve data collection with excitation pulse energies that were low enough to avoid multiphoton events. Our goal was to establish, as best possible, characteristic absorption spectra of the transient bathorhodopsin photoproducts arising from 11-*cis*- and 9-*cis*-rhodopsin at room temperature and to compare these with the published spectra obtained by photostationary studies carried out with aqueous glycerol/rhodopsin glasses at low temperature.

METHODS AND MATERIALS

Visual Pigment Samples. Buffer is defined throughout this work as 0.01 M HEPES, pH 7/0.1 mM EDTA/1.0 mM dithiothreitol. Rhodopsin was prepared from frozen bovine retinae (G. Hormel), solubilized in Ammonyx-LO detergent, and purified by hydroxyapatite chromatography (1, 2). The relative purity of the samples used is indicated by the ratio $A_{278}/A_{498} = 1.9 \pm 0.1$. For preparation of regenerated 9-*cis*-rhodopsin, the 9-*cis*-retinaldehyde isomer was made by photolysis of *all-trans*-retinal (Fluka, Buchs, Switzerland) dissolved in trifluoroethane, with appropriately filtered light (Schott 06455 and 06745). 9-*cis*-Retinal was isolated by preparative HPLC and was found to be >99% pure by analytical HPLC. The retinal was stored at -70°C under N_2 until incorporated into opsin. 9-*cis*-Rhodopsin was prepared from opsin, made by washing bleached disk membranes with buffered NH_2OH , and

purified 9-*cis*-retinal. The regenerated pigment was solubilized and purified by hydroxyapatite chromatography (1, 2). The relative purity is indicated by the ratio $A_{278}/A_{485} = 1.8 \pm 0.1$. The purified 9-*cis*-rhodopsin was shown to contain the 9-*cis*-retinal isomer by HPLC. The molar extinction coefficients used throughout this work were $\epsilon_{11}^r(498 \text{ nm}) = 4.06 \times 10^4 \text{ M}^{-1}\text{cm}^{-1}$ for 11-*cis*-rhodopsin (1, 3) and $\epsilon_9^r(485 \text{ nm}) = 4.3 \times 10^4 \text{ M}^{-1}\text{cm}^{-1}$ for 9-*cis*-rhodopsin (4, 5).

Picosecond Spectroscopy. Spectral changes were observed by a double-beam laser spectrophotometer constructed on the design of Netzel and Rentzepis (6) with the following modifications. The rhodopsin samples were photoexcited by a single, 25-psec (FWHM) light pulse at 532 nm, which was generated by a KDP crystal from the 1064-nm pulse emitted by a neodymium(III)/yttrium–aluminum garnet ($\text{Nd}^{3+}/\text{YAG}$) laser (Quantel, Santa Clara, CA). The absorbance changes were monitored by a broad-band picosecond continuum generated in a 10-cm quartz cuvette containing water. Scattered light from the excitation pulse was blocked from entering the monitoring pathway by a narrow-band rejection filter constructed by Omega Optical (Brattleboro, VT). This filter allowed us to monitor absorbance over the entire wavelength range and to avoid problems related to the use of cross-polarizers in excitation and monitoring pathways.

Samples (50 μl) were monitored in a quartz flow cell of 2-mm path length (Hellma 138 QS). A maximum of two records were taken with one sample. At the excitation energies used, the amplitudes and the shapes of the difference spectra differed by <5% between first and second shots. Experiments were performed under as nearly identical conditions as possible for 11-*cis*- and 9-*cis*-rhodopsin samples.

The spectral information of both the probe $a(\lambda)$ and reference $a_o(\lambda)$ beams was collected for a pair of shots with no excitation (no) and excitation (ex). Difference spectra were then calculated for each of these pairs according to

$$\Delta A(\lambda) = -\log_{10} \left[\frac{\left(\frac{a^{\text{ex}}(\lambda)}{a_o^{\text{ex}}(\lambda)} \right)}{\left(\frac{a^{\text{no}}(\lambda)}{a_o^{\text{no}}(\lambda)} \right)} \right]$$

Data such as those given in Figs. 2–5 represent averages of several pairs.

RESULTS

Rhodopsin samples were purified to remove free unbound retinal that might interfere with visual pigment absorption and were solubilized for high optical clarity to minimize light scattering. The rate of production of bathorhodopsin (2, 7, 8), the low temperature spectra (1, 8–11), and the quantum yield of bleaching (12–14) are the same whether rhodopsin is solu-

The publication costs of this article were defrayed in part by page charge payment. This article must therefore be hereby marked "advertisement" in accordance with 18 U. S. C. §1734 solely to indicate this fact.

[†]To whom reprint requests should be addressed.

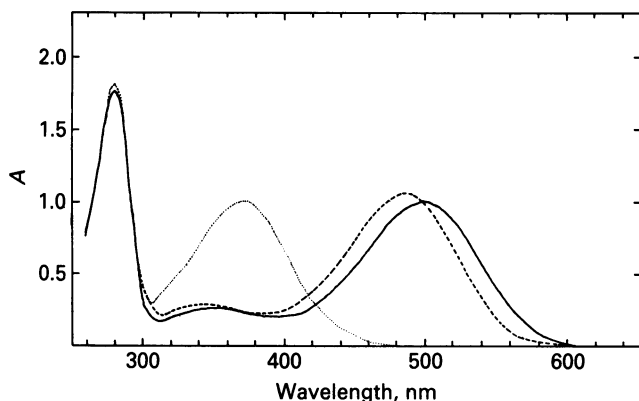


FIG. 1. Absorption spectra of native 11-*cis*-rhodopsin and regenerated 9-*cis*-rhodopsin. Spectra were taken on a Varian 219 spectrophotometer (1-cm path length). —, 11-*cis*-Rhodopsin; ---, 9-*cis*-rhodopsin; ·····, bleached 11- or 9-*cis*-rhodopsin. The absorbances are normalized to the absorbance maximum of 11-*cis*-rhodopsin, $40,600 \text{ M}^{-1} \text{ cm}^{-1}$ (3) at 498 nm.

bilized or in its native membrane environment. A change is noticed in the circular dichroism spectrum of the β -chromophore band (14, 15), however, and the kinetics of bleaching at later stages do differ (1). The electronic absorption spectra of solubilized 11-*cis*- and 9-*cis*-rhodopsin are compared in Fig. 1. The characteristic rhodopsin absorption bands are shifted to the blue for the regenerated 9-*cis* visual pigment. Note that for samples of similar molarity used in these studies, the absorption of 11-*cis*-rhodopsin was ≈ 1.5 times that of 9-*cis*-rhodopsin at the 532-nm excitation wavelength.

Difference Spectra Generated at 85 psec. An initial study of the difference spectra of the bathorhodopsin produced minus the rhodopsin bleached is shown in Fig. 2 *a* and *b*. For comparison of spectra, extensive data-averaging was carried out. The signal-to-noise ratio was adequate enough to show that the isosbestic point of the 11-*cis*-rhodopsin spectrum (≈ 520 nm) was shifted to the red by about 5 nm compared to that

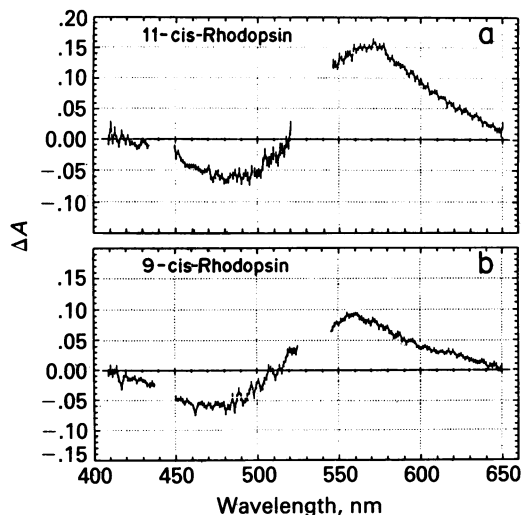


FIG. 2. Bathorhodopsin-rhodopsin difference spectra measured 85 psec after excitation. Spectra were taken at room temperature; sample concentrations gave absorbances of $1.0 A_{498 \text{ nm}}$ and $1.0 A_{485 \text{ nm}}$ (2-mm path length) for 11-*cis*- and 9-*cis*-rhodopsins, respectively. The excitation pulse fluence corresponds to one-half to three relative units in Fig. 3. (a) Spectrum of bathorhodopsin minus that of 11-*cis*-rhodopsin; 58 averaged records. (b) Spectrum of bathorhodopsin minus that of 9-*cis*-rhodopsin; 55 averaged records.

of 9-*cis*-rhodopsin (≈ 515 nm). There was no indication of positive absorption in the region of 400–450 nm. The difference spectra indicate that the ratio of maximum absorption arising from bathorhodopsin production ($\Delta\lambda_{\text{max}}$) to minimum absorption arising from rhodopsin bleached ($\Delta\lambda_{\text{min}}$) is ≈ 2.3 for the 11-*cis* and ≈ 1.5 for the 9-*cis* form. The ratio for the 11-*cis* form was more than 2-fold higher than that previously measured at room temperature (16, 17) but was nearly the same as that measured after photolysis of rhodopsin at low temperatures (1, 5, 8, 9, 11). To insure that the difference spectra observed were proportional to the photons absorbed and free from multiphoton effects, we studied spectra over a range of excitation energies.

11-*cis*-Rhodopsin and 9-*cis*-Rhodopsin Exhibit Different Photon Saturation Properties. Plots of difference spectra at $\Delta\lambda_{\text{max}}$ and $\Delta\lambda_{\text{min}}$ vs. excitation pulse energies are shown in Fig. 3. Four to six single records were averaged for each excitation energy plotted. The geometry of excitation vs. monitoring pulse (coincident within 5°) dictates that the measured absorbance change should show an exponential dependence [of the form $1 - \exp(x)$] upon excitation pulse energy (18, 19). The saturation plots of Fig. 3 are consistent with an exponential dependence at low fluence and reveal that (i) equal excitation energies resulted in similar $\Delta\lambda_{\text{min}}$ for the 11-*cis* and 9-*cis* forms, but (ii) 11-*cis*-rhodopsin showed a larger $\Delta\lambda_{\text{max}}$, corresponding to bathorhodopsin production, which became saturated at lower excitation-pulse energies than in the case of 9-*cis*-rhodopsin.

By comparing difference spectra at low, medium, and high excitation energies (Fig. 4), one also notes that 11-*cis*-rhodopsin became saturated (apparently because of multiple photon processes) at relatively low energy levels. The spectra averaged over the lowest energies (Fig. 4a, LOW spectrum), resulted in a difference spectrum that shows a $\Delta A_{570}/\Delta A_{490}$ ratio of 3.0. This ratio differs from previously published ratios, which were obtained by picosecond spectroscopy and which are as low as 1.0 (8, 16, 17), but agrees with results of low-temperature experiments carried out in aqueous glasses at 4 K (8). In addition, the difference spectra for 11-*cis*-rhodopsin clearly showed a shift of the isosbestic point towards shorter wavelengths upon going from high to low excitation

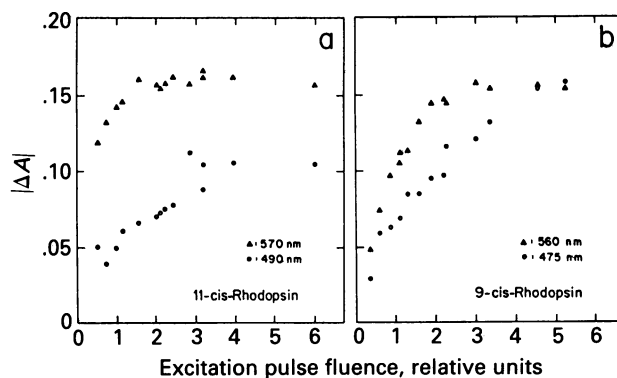


FIG. 3. Absorbance change at λ_{max} (▲) or λ_{min} (○) as a function of excitation fluence. The experimental conditions are as in Fig. 2. Each point represents the average of 4–6 single records for similar excitation energies, which were measured with a new energy meter (RJ5200, Laser Precision, Yorkville, NY) calibrated against the standard from the National Bureau of Standards. One relative unit corresponds to between 10–35 $\mu\text{J}/\text{mm}^2$. The maximum energy used was 1 mJ for a beam area $\approx 16 \text{ mm}^2$. (a) Bathorhodopsin minus 11-*cis*-rhodopsin spectral amplitudes at 570 nm (▲) and 490 nm (○). (b) Bathorhodopsin minus 9-*cis*-rhodopsin spectral amplitudes at 560 nm (▲) and minimum at 475 nm (○).

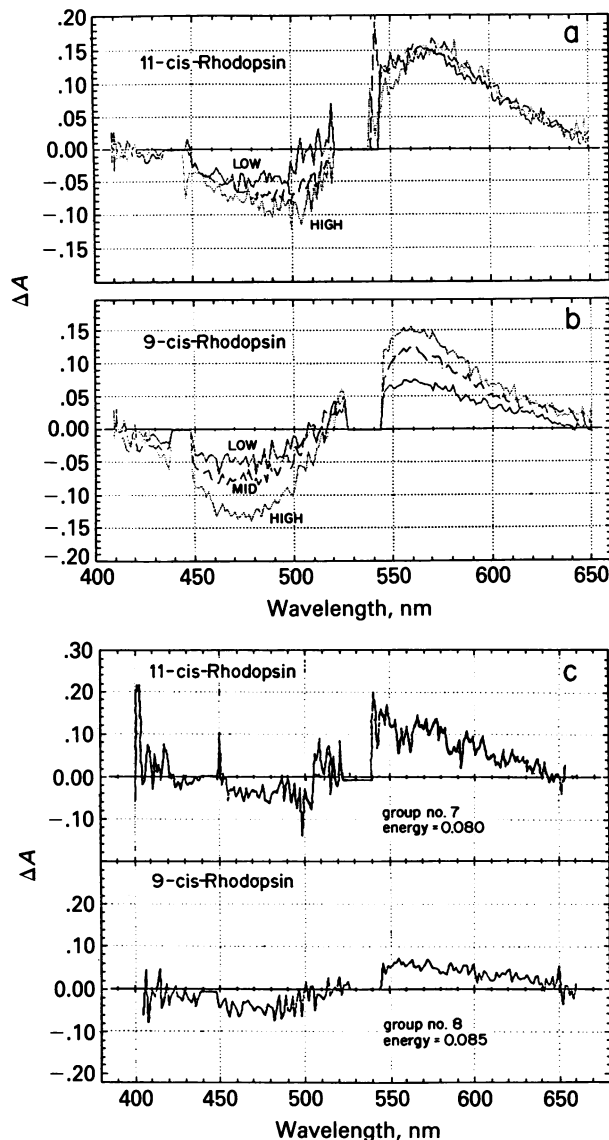


FIG. 4. Dependence of difference spectra on excitation energy. The experimental conditions directly correspond to those in Figs. 2 and 3. The spectra represent averages of data grouped into three excitation fluence ranges in accordance with Fig. 3a. LOW, less than two relative units; MID, two to three relative units; and HIGH, more than three relative units. (a) Bathorhodopsin spectrum minus that of 11-*cis*-rhodopsin. (b) Bathorhodopsin spectrum minus that of 9-*cis*-rhodopsin. (c) Comparison of difference spectra at low fluences. The data are not averaged. Total spectral energies are $\approx 80 \mu\text{J}$ for the 11-*cis* form and $\approx 85 \mu\text{J}$ for the 9-*cis* form for an $\approx 16\text{-mm}^2$ excitation beam.

energies (Fig. 4a). For 9-*cis*-rhodopsin, there was little indication of multiphoton effects until a higher region of excitation energies was reached (Fig. 3b). The difference spectra for 9-*cis*-rhodopsin showed a ratio of $\Delta A_{560}/\Delta A_{475} = 1.5 \pm 0.1$ and an isobestic point of $515 \pm 3 \text{ nm}$, which did not change significantly over the excitation energy range.

The data shown in Fig. 4c were taken at ≈ 0.5 relative fluence units (see Fig. 3), where there were < 0.2 photons per molecule of rhodopsin, and simulated calculations indicated that multiphoton absorptions cannot be significant. Although the signal-to-noise ratio was poor, it could be seen that the negative ΔA (proportional to the rhodopsin bleached) was nearly the same for the 11-*cis* and 9-*cis* forms, and the maximal ΔA (proportional to the bathorhodopsin produced) was significantly larger for 11-*cis* than for 9-*cis* forms. In summary, Fig.

4 a-c shows two notable features: (i) At high energies the isobestic point of the 11-*cis*-rhodopsin spectrum is shifted to the red by $\approx 10 \text{ nm}$ compared to that in the 9-*cis*-rhodopsin spectrum, but at low energies it becomes equivalent or even shifted to the blue, and (ii) the ratio of $\Delta\lambda_{\text{max}}$ to $\Delta\lambda_{\text{min}}$ is dependent on energy for 11-*cis*-rhodopsin but relatively independent of energy for 9-*cis*-rhodopsin.

Sets of data were collected at 600-psec and 8-nsec delays between excitation and observation in the low-energy range (unpublished data). The spectra were identical to the LOW spectra given in Fig. 4 a and b, respectively, and reveal no changes in the state of intermediates on the timescale up to 8 nsec.

Relative Quantum Yields of 11-*cis*/9-*cis*-Forms of Bathorhodopsin. The above observations suggested that 9-*cis*-bathorhodopsin produced at room temperature does not behave as predicted from earlier studies, particularly photostationary studies carried out at low temperatures. For instance, the quantum yield for 11-*cis*-bathorhodopsin is 0.67 and is independent of wavelength and temperature (12, 13, 20); that for 9-*cis*-bathorhodopsin has been given as 0.3 at room temperature (21, 22) and 0.1–0.2 at 77 K (20, 23, 24). At 532 nm, the absorption for 11-*cis*- was greater than for 9-*cis*-bathorhodopsin; thus, at any given excitation energy, the amplitudes of 11-*cis*-bathorhodopsin difference spectra would be expected to be greater than those in the case of the 9-*cis*-bathorhodopsin. The observed $\Delta\lambda_{\text{min}}$, however, were for the most part equivalent and the $\Delta\lambda_{\text{max}}$ were within a 2-fold range (Fig. 3). The photon saturation effects occurred at 2-fold higher energies for 9-*cis*- than for 11-*cis*-bathorhodopsin. Although production of less bathorhodopsin from 9-*cis*-rhodopsin per given photon fluence would be consistent with a saturation at higher energies, lower production is not consistent with the $\Delta\lambda_{\text{min}}$ in the region of 470–490 nm (Fig. 4 a-c, spectrum LOW). Thus, we attempted to compare qualitatively the quantum yields for 11-*cis*- and 9-*cis*-rhodopsin in the energy range producing the LOW spectra.

An average percentage bleach may be determined by pooling several samples used for transient measurements and recording the average post-bleach absorption at which time (min) bathorhodopsin has converted to retinal and opsin. The excitation energies were averaged for 55 records of 11-*cis*-rhodopsin, whose starting $A_{532}^{2 \text{ min}} = 0.70$ and 25 records of 9-*cis*-rhodopsin whose $A_{532}^{2 \text{ min}} = 0.45$. The percentage of bleach, measured for an average 200- μJ incident energy, was 8.7% for 11-*cis*-rhodopsin and 8.0% for 9-*cis*-rhodopsin. The irradiated area of the sample cell was equivalent for both samples so that the fluence corresponded to the region of < 2 relative fluence units (Fig. 4 a and b). Bathorhodopsin produced (i.e., rhodopsin bleached) may be given as $\beta_i = \phi_i^b I_a = \phi_i^b I_o$ ($1 \cdot 10^{-A_{532 \text{ nm}}}$) in which ϕ_i^b is the quantum yield of bathorhodopsin formed, I_a is the number of photons absorbed, and I_o is the initial excitation fluence. Because the bleach was measured under equivalent conditions (I_o) for the 11-*cis* and 9-*cis* forms, the ratio of quantum yields $\phi_{11}^b/\phi_9^b = 0.9 \pm 0.3$. Because of spatial inhomogeneities, specific quantum yields were difficult to determine. The excitation beam was spread to cover $> 90\%$ of the sample, but inhomogeneity could give higher bleaches in a local interrogation area. We estimate an upper limit of 3 times the $\approx 8\%$ measured bleach could sometimes occur, but the ratio of bleaches for 11-*cis*- and 9-*cis*-rhodopsin should not change. Thus, the data collected here suggest that the quantum yields for batho products from 11-*cis*- and 9-*cis*-rhodopsin are approximately equivalent and are inconsistent with values for 9-*cis*-bathorhodopsin as low as 0.1–0.2 (20, 21, 24).

Table 1. Bathorhodopsin spectra resolved from difference spectra taken at 85 psec after excitation

Case	% bleach		Bathorhodopsin spectral characteristics at 298 K				ϕ_{11}/ϕ_9	$[\chi^2/f_n]^{1/2}$
	β_{11}	β_9	$(\lambda_{\max})_{11}$	$\bar{\epsilon}_{11}^b$	$(\lambda_{\max})_9$	$\bar{\epsilon}_9^b$		
I	$\bar{\epsilon}_{11}^b = \bar{\epsilon}_9^b$	31 13	517	0.93	517	0.93	1.9	1.9
II	$\bar{\epsilon}_{11}^b = n\bar{\epsilon}_9^b$	19 10	535	1.10	535	0.92	1.6	1.6
III	$\bar{\epsilon}_{11}^b \neq \bar{\epsilon}_9^b$	15 13	545	1.20	535	0.90	0.9	—

Cases are defined in the text. The error in $(\lambda_{\max})_i$ is $\approx 3\%$ and in other values is $\approx 25\%$. Bathorhodopsin spectra were resolved by using a variable multiparameter regression analysis with the following equations:

$$\bar{\epsilon}_{11}^b(\lambda) = \bar{\epsilon}_{11}^r(\lambda) + \Delta A_{11}(\lambda)/\beta_{11} \cdot a_{11}(498)$$

$$\bar{\epsilon}_9^b(\lambda) = \bar{\epsilon}_9^r(\lambda) + \alpha \Delta A_9(\lambda)/\beta_9 \cdot a_9(485)$$

$$\chi^2 = \sum_{\lambda} \frac{[\bar{\epsilon}_{11}^b(\lambda) - n\bar{\epsilon}_9^b(\lambda)]^2}{\delta_{11}^2(\lambda) + n^2 \delta_9^2(\lambda)}$$

A, absorbance in which $\bar{\epsilon}_i(\lambda)$ is the extinction coefficient normalized to $\bar{\epsilon}_{11}^r(498) = 4.06 \times 10^4 \text{ M}^{-1} \text{ cm}^{-1}$; ΔA , difference spectrum amplitude; β , % bleach; $a_i(\lambda)$, absorption of pigment photolyzed for 2-mm path; λ , wavelength; $\alpha = \bar{\epsilon}_9^r(485)/\bar{\epsilon}_{11}^r(498) = 1.06$; $\delta_i^2(\lambda)$, variance in each value; f_n , number of points (λ) summed; and ϕ_i , quantum yield for bathorhodopsin. The indices are: r, rhodopsin; b, bathorhodopsin; 11, 11-*cis*-rhodopsin; 9, 9-*cis*-rhodopsin. For cases I and II, a wide survey was made for bleaches ranging from 5% to 40% for LOW spectra from Fig. 4a and b. A refined analysis was then made in the region of best fit (lowest χ^2). The program for regression analysis was written in Fortran for Data General Eclipse S/130 minicomputer. The program and spectral fits are available from A.H.R.

Bathorhodopsins from 11-*cis*- and 9-*cis*-Rhodopsins Differ.

By assuming a percentage of bleach, we can approximate the bathorhodopsin spectra at room temperature. Table 1 indicates the results of the computer analyses carried out to resolve the difference spectra under the following conditions: (case I) bathorhodopsins generated from 11-*cis*- or 9-*cis*-rhodopsin were defined as equivalent and the percentage of bleach was varied independently for 11-*cis*- and 9-*cis*-rhodopsins until regression analyses indicated the best possible fit was achieved; (case II) bathorhodopsins from 11-*cis*- and 9-*cis*-rhodopsins were defined to have the same shape (λ_{\max} and relative width), but the absolute value for the extinction coefficient was allowed to vary by some factor until a reasonable fit was achieved; and (case III) bathorhodopsins were generated by selecting various bleach percentages between the limits of 8% and 30%. In this latter case, data are given for midpoints of 15% and 13% bleach for 11-*cis*- and 9-*cis*-rhodopsin and for the relative ratio of quantum yields that were measured above. All analyses were carried out by using the difference spectra designated LOW in Fig. 4a and b, for which the average excitation energy was equivalent for the 11-*cis*- and 9-*cis*-rhodopsin samples.

Most of the reasonably possible bathorhodopsin spectra are covered by these analyses. Case I seems unlikely because it demands a percentage of bleach that is unduly high for 11-*cis*-rhodopsin and a ratio of bleaches (β_{11}/β_9) that is inconsistent with the ratio of average bleaches measured. Although a common intermediate bathorhodopsin can be found, the goodness of fit is poor, reflecting differences in bandwidth. Case II is also less than optimal in fit, and the ratio of bleaches again differs from that observed. Case III is consistent with the limits of bleaching and the observed bleaching ratios. The spectra for this case are shown in Fig. 5. Comparison of these approximate spectra indicates that (i) the λ_{\max} for bathorhodop-

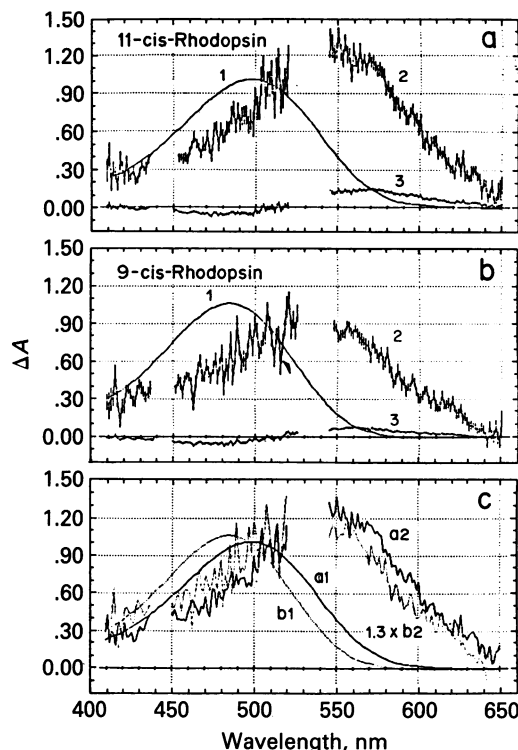


FIG. 5. Approximation of bathorhodopsin spectra at 298 K 85 psec after excitation. Calculated bathorhodopsin absorption spectra corresponding to Table 1, case III. (a) Spectra: 1, parent 11-*cis*-rhodopsin spectrum; 2, computed spectrum of bathorhodopsin from 11-*cis*-rhodopsin, resolved from curve 3 by assuming a 15% bleach; 3, LOW spectrum from Fig. 4a. (b) Spectra: 1, parent 9-*cis*-rhodopsin spectrum; 2, computed spectrum of bathorhodopsin from 9-*cis*-rhodopsin, resolved from curve 3 by assuming a 13% bleach; 3, LOW spectrum from Fig. 4b. (c) Comparison of the two calculated bathorhodopsin spectra (spectra 2 in a and b) scaled to the same maximum absorption, shows the spectral shift between pigments. Curve 1 in a and b, respectively, is the 11-*cis*- and 9-*cis*-rhodopsin spectrum.

sin generated from 9-*cis*-rhodopsin is shifted ≈ 10 nm to the blue compared with that from 11-*cis*-rhodopsin, and (ii) the extinction coefficient for the bathorhodopsin from 9-*cis*-rhodopsin is lower than that from 11-*cis*-rhodopsin.

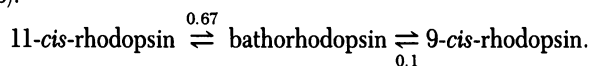
DISCUSSION

A careful study of the production of bathorhodopsin as a function of excitation energy indicates that multiphoton events are a serious problem in the study of primary photochemical events in vision. This is particularly so for picosecond spectroscopy because until recently excitation has been experimentally limited to 532 nm (or other harmonics of the yttrium-aluminum garnet laser's 1,064-nm output), a wavelength at which both rhodopsin and its photoproduct absorb. A study of difference spectra of bathorhodopsin generated from 11-*cis*-rhodopsin at 298 K 85 psec after excitation indicates that the earlier observed discrepancy in 298 K spectra compared with those taken at 77–4 K (3, 16, 17, 25) can be explained by saturation effects (Fig. 3). At low-excitation energies, the ratio of $\Delta\lambda_{\max}$ to $\Delta\lambda_{\min}$ in difference spectra is the same at room temperature and low temperature, ranging from 2.7–3.1 (refs. 1, 10, and 11; Fig 4a, LOW spectra). Because the spectrum of rhodopsin is redshifted to 505 nm, the half-width is narrowed, and the λ_{\max} extinction is increased at 4–77 K as compared with spectra at room temperature (1, 5, 10), such effects might be expected for bathorhodopsins as well. Table 1 and Fig. 5 do indicate

that the room-temperature spectra are broader and have lower extinction than the low-temperature spectra given in the literature (5, 10, 26).

The cause of saturation observed in Fig. 3 is unknown. At two relative fluence units ($\approx 3 \text{ mJ/cm}^2$), such multiphoton events as two-photon absorption or rhodopsin excited-state absorption are unlikely. A model in which bathorhodopsin is allowed to absorb a second photon, driving it to some unknown species X, can explain the observed saturation. For our conditions, such events become significant at $\approx 4 \text{ mJ/cm}^2$ for a 532-nm excitation pulse. In this model, X could not be equivalent to rhodopsin or isorhodopsin because no change in the ratio of maximal to minimal absorbance in the difference spectra would then be observed, in contrast to data in Fig. 4a. This model could explain the earlier discrepancy between room-temperature and low-temperature data. In these earlier studies, bathorhodopsin was produced at room temperature within a ≈ 6 -psec excitation pulse (7) and could have been driven photolytically to some other state; at low temperature, the rise-time of bathorhodopsin is ≈ 36 psec (8) so that it would not be present in significant concentration during excitation to absorb. Other models also may explain the saturation, and further investigation is needed to clarify our observations.

Photostationary studies of rhodopsin-bathorhodopsin at low temperature have been accounted for by a model that suggests that the following photoequilibrium is established (10, 20, 24, 26):



This mechanism, which assumes a common bathorhodopsin, has been one of the key paradigms dictating that the primary event in vision is *cis-trans* isomerization. However, the study of these two rhodopsins at room temperature under limiting photon fluxes indicates that the respective bathorhodopsins differ when observed as transients between 85 psec and 8 nsec, and the quantum yield for 9-*cis*-bathorhodopsin is 3- to 6-fold higher. For low-temperature experiments, no study has been published that systematically examines the excitation fluence range over which photoproduct production is exponentially dependent on photons absorbed. Published spectra may or may not be subject to saturation or multiphoton effects, or both. Alternatively, modes of protein relaxation (see below) that affect the chromophore environment may differ between 298 K and 4–77 K.

Presumably each of the bathorhodopsins generated from 11-*cis*- and 9-*cis*-rhodopsin have a transoid chromophore, but these must differ somehow in distortion or the protein binding site must differ at this early state of bleaching, or both. Although not yet demonstrated, it seems possible that the protein could be pliable and that the pocket which binds 11-*cis*-retinal might conform to the 9-*cis*-retinal in an altered fashion. In such a case, early intermediates involving modest protein relaxations might not be expected to be similar.

Upon photon absorption, some degree of deformation in the *cis*-retinaldehyde must take place to commit the chromophore to a batho intermediate that ultimately decays to the relaxed *all-trans* state and to allow for the observed proton translocation (8). Broad unstructured electronic spectra are poor indications of what this structural deformation might be. The difference in spectra between bathorhodopsins from 11-*cis*- and 9-*cis* rhodopsin (Fig. 4 a and b), as well as resonance Ra-

man studies of 11-*cis*-bathorhodopsin (27–30), suggest that the chromophore has a distorted *trans* structure. Our observations emphasize that there is not a common bathorhodopsin state produced from 11-*cis*- or 9-*cis*-rhodopsin. Perhaps this subtlety only dictates a need for a better description of the chromophore site and a need for knowledge of contributions the protein must make in determining the spectral intermediates—hence, in controlling the primary photochemical process.

The authors wish to thank Wolfgang Baehr and Kathy Savoie-Luisi for their expert help in preparation of rhodopsin samples. We thank K. S. Peters for initiating preliminary experiments and for his continued interest in this work. This work was supported in part by a grant from the Deutsche Forschungsgemeinschaft to J.D.S. and a grant from the National Eye Institute to M.L.A.

1. Applebury, M. L., Zuckerman, D. M., Lamola, A. A. & Jovin, T. M. (1974) *Biochemistry* 13, 3448–3458.
2. Applebury, M. L. & Rentzepis, P. M. (1982) *Methods Enzymol.* 81, 354–368.
3. Wald, G. & Brown, P. K. (1953) *J. Gen. Physiol.* 37, 189–200.
4. Hubbard, R. J. (1956) *J. Gen. Physiol.* 39, 935–962.
5. Yoshizawa, T. (1972) in *Handbook of Sensory Physiology*, ed. Dartnall, H. J. A. (Springer, Berlin), Vol. 7, Part 1, pp. 146–179.
6. Netzel, T. L. & Rentzepis, P. M. (1974) *Chem. Phys. Lett.* 29, 337–342.
7. Busch, G. E., Applebury, M. L., Lamola, A. A. & Rentzepis, P. M. (1972) *Proc. Natl. Acad. Sci. USA* 69, 2802–2806.
8. Peters, K., Applebury, M. L. & Rentzepis, P. M. (1977) *Proc. Natl. Acad. Sci. USA* 74, 3119–3123.
9. Grellman, K.-H., Livingston, R. & Pratt, O. (1962) *Nature (London)* 193, 1258–1260.
10. Yoshizawa, T. & Wald, G. (1963) *Nature (London)* 197, 1279–1286.
11. Tokunaga, F., Kawamura, S. & Yoshizawa, T. (1976) *Vision Res.* 16, 633–641.
12. Dartnall, H. J. A. (1972) in *Handbook of Sensory Physiology*, ed. Dartnall, H. J. A. (Springer, Berlin), Vol. 7, Part 1, pp. 122–145.
13. Dartnall, H. J. A. (1968) *Vision Res.* 8, 339–358.
14. Waddell, W. H., Yudd, A. P. & Nakanishi, K. J. (1976) *J. Am. Chem. Soc.* 98, 238–239.
15. Ebrey, T. G. & Yoshizawa, T. (1973) *Exp. Eye Res.* 17, 545–556.
16. Sundstrom, V., Rentzepis, P., Peters, K. & Applebury, M. L. (1977) *Nature (London)* 267, 645–646.
17. Monger, T. G., Alfano, R. R. & Callender, R. H. (1979) *Biophys. J.* 27, 105–116.
18. Hartmann, K. M. & Unser, I. C. (1972) *Ber. Dtsch. Bot. Ges.* 85, 481–551.
19. Peretti, P., Ranson, P. & Rousset, V. (1973) *Opt. Commun.* 9, 106–111.
20. Hurley, J. B., Ebrey, T. G., Honig, B. & Ottolenghi, M. (1977) *Nature (London)* 270, 540–542.
21. Hubbard, R. & Kropf, A. (1958) *Proc. Natl. Acad. Sci. USA* 44, 130–139.
22. Kropf, A. & Hubbard, R. (1958) *Ann. N.Y. Acad. Sci.* 74, 266–280.
23. Rosenfeld, T., Honig, B., Ottolenghi, M., Hurley, J. & Ebrey, T. G. (1977) *Pure Appl. Chem.* 49, 341–351.
24. Susuki, T. & Callender, R. H. (1981) *Biophys. J.* 34, 261–265.
25. Applebury, M. L. (1980) *Photochem. Photobiol.* 32, 425–431.
26. Mao, B., Ebrey, T. G. & Crouch, R. (1980) *Biophys. J.* 29, 247–256.
27. Oseroff, A. R. & Callender, R. H. (1974) *Biochemistry* 13, 3243–3248.
28. Sulkes, M., Lewis, A. & Marcus, M. A. (1978) *Biochemistry* 17, 4712–4722.
29. Aton, B., Doukas, A. G., Narva, D., Callender, R. H., Dinur, U. & Honig, B. (1980) *Biophys. J.* 29, 79–94.
30. Eyring, G., Curry, B., Mathies, R., Fransen, R., Palings, I. & Lugtenburg, J. (1980) *Biochemistry* 19, 2410–2418.